

Probing dark matter distribution with gravitational lensing and stellar dynamics

Tommaso Treu & Léon V. E. Koopmans
California Institute of Technology
Astronomy 105-24
Pasadena, CA 91101, USA



The Lenses Structure and Dynamics (LSD) Survey aims at measuring the luminous and dark matter distribution of high redshift early-type galaxies by combining gravitational lens analysis with newly determined velocity dispersion profiles. Here we describe the first results from the LSD survey, a measurement of the internal structure of the lens galaxy in MG2016+112 ($z = 1.004$). The relevance of this measurement to the cosmological model is briefly discussed, in particular in the context of E/S0 galaxy formation and evolution, the existence and shape of universal dark matter profiles, and the measurement of the Hubble constant from gravitational time delay.

1 Introduction

Little is known about the distribution of mass in early-type galaxies (E/S0). In fact, the paucity of kinematic tracers at large radii (beyond the effective radius R_e , i.e. beyond the region dominated by stellar mass) severely limits the information that can be inferred by dynamical studies. In the local Universe, particularly accurate and extensive data have provided evidence for the existence of dark-matter halos in E/S0, with constraints on the shape of the dark matter distribution. At higher redshifts, galaxy-galaxy lensing and strong lensing have provided independent confirmation for the existence of dark halos, and some information on the mass distribution.

The aim of the Lenses Structure and Dynamical (LSD) Survey is to measure the luminous and dark matter distribution of E/S0, by combining lensing and kinematic constraints. The combination of these two diagnostics provides independent constraints on the same physical length-scales, effectively removing degeneracies inherent to each method alone (such as that between anisotropy and mass in kinematic studies). In particular, this technique allows us to study in detail the distribution of luminous and dark matter in E/S0 at significant look-back time (up to ~ 8 Gyrs) with accuracy comparable to studies in the local Universe. In practice, we

are measuring (using the Echellette Spectrograph and Imager ESI at the 10m Keck-II Telescope) velocity dispersion and streaming motion profiles of a sample of 11 lens E/S0 ($0 < z < 1$), chosen to be relatively clean systems, covering uniformly the redshift range, and spanning the widest possible range in masses (a more detailed description of the survey is given in Treu & Koopmans¹⁷, hereafter TK02).

The relevance of this study to this conference is two-fold. First of all, as described in the opening review by Jim Peebles, the formation of early-type galaxies is a very controversial but interesting issue because it provides a crucial observational constraint on cosmological models. Most of the studies on E/S0 at intermediate and high redshift so far were concerned with the evolution of the stellar populations. The LSD Survey provides additional valuable and detailed information on the internal structure of high redshift E/S0 and hence on its evolution. Second, Cold Dark Matter (CDM) cosmological simulations find that dark matter halos have a universal density profile (see the next section), characterized by a cuspy inner slope. This prediction has been challenged by the observation of soft cores in local dwarf and low surface brightness galaxies (but see review talk by Simon White). The LSD Survey provides a completely independent determination of the shape of dark matter halos in massive E/S0 galaxies— at different mass scales, physical conditions, and look-back time.

2 A Case study: MG2016+112 at $z = 1$

In this contribution we focus in particular on the first object analyzed by our survey. The lens galaxy in MG2016+112 is the most distant spectroscopically confirmed lens ($z = 1.004$) and therefore offers the possibility of exploring the internal structure of an E/S0 at a significant look back-time (~ 8 Gyr in the assumed cosmology $\Omega_m = 0.3$, $\Omega_\Lambda = 0.7$, $H_0 = 65 \text{ km s}^{-1} \text{ Mpc}^{-1}$). In addition, the Einstein radius is almost five times the effective radius (see below) and therefore the mass profile is constrained out to the largest radii probed even in local E/S0, yielding a robust determination of the slope of the total mass distribution. Due to the extreme faintness and distance of MG2016+112, only a luminosity-weighted velocity dispersion was measured, and therefore no tight constraints on the orbital structure of the system could be placed (see Koopmans & Treu⁹ for the analysis of a system with spatially resolved kinematics and constraints on the velocity ellipsoid).

2.1 Observations and modeling

The lens galaxy in MG2016+112 was imaged with the Hubble Space Telescope. Surface photometry (Koopmans & Treu⁸; hereafter TK02a) shows that the surface brightness profile is well-fit by a de Vaucouleurs profile with effective radius $R_e = 0.31'' \pm 0.06''$, i.e. 2.7 ± 0.5 kpc. We observed MG2016+112 using ESI on the W.M. Keck-II Telescope during four consecutive nights (23–26 July, 2001), with a total integration time of 8.5 hrs. The region around the absorption G-band (Fig 1) was used to derive a velocity dispersion of $\sigma_{\text{ap}} = 304 \pm 27 \text{ km s}^{-1}$ inside an effective circular aperture with radius $0.65''$, corresponding to a central velocity dispersion (i.e. measured in a $R_e/8$ aperture) of $\sigma = 328 \pm 32 \text{ km s}^{-1}$. Details of the measurement are given in KT02a.

We can use these measurements to determine the offset of the galaxy with respect to the local Fundamental Plane (Djorgovski & Davis³ Dressler et al.⁴) and therefore measure the evolution of the effective mass to light ratio (Figure 1 right panel; see Treu et al.¹⁸ and KT02a for discussion). Assuming, as in TK02, that the evolution of the effective mass to light ratio is equal to the evolution of the stellar mass to light ratio, we can use this measurement to predict the stellar mass-to-light ratio of MG2016+112 finding $M_*/L_B = 1.8 \pm 0.7$ in solar units.

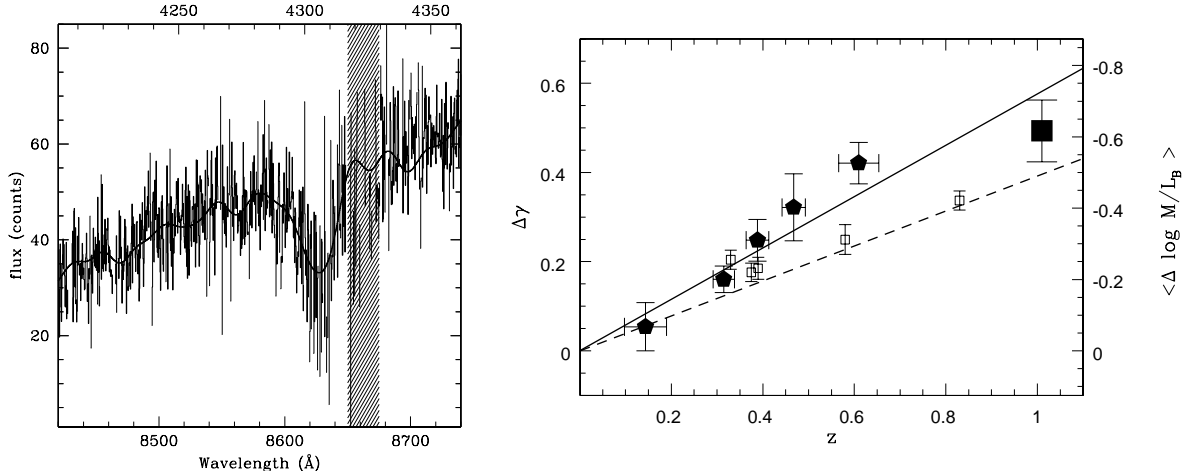


Figure 1: Left: the G-band absorption feature in the spectrum of MG2016+112. The rest-frame wavelength scale is shown on the top axis for reference. The smooth solid line is the best-fitting template (spectral-type G4–III) broadened to the measured velocity dispersion $\sigma_{\text{ap}} = 304 \pm 27 \text{ km s}^{-1}$. The dashed region is affected by sky-subtraction residuals and was omitted in the fit. Right: Evolution of the M/L as inferred from the evolution of the FP. Filled pentagons and open squares represent field and cluster measurements, respectively, while the thick full and dashed lines indicate linear fits to the M/L evolution for field and cluster E/S0 (see Treu et al. 2002 for details). The large filled square at $z = 1.004$ indicates the M/L evolution of MG2016+112.

Finally, the lens configuration provides an accurate measurement of the mass enclosed by the Einstein Radius (13.7 kpc), $M_E = 1.1 \times 10^{12} M_\odot$ (Koopmans et al. ¹¹).

The galaxy mass distribution is modeled as a superposition of two spherical components, one for the luminous stellar matter and one for the dark-matter halo. The luminous mass distribution is described by a Hernquist (1990) model, which provides a good analytical approximation to the luminous component of early-type galaxies. The dark-matter distribution is modeled as

$$\rho_d(r) = \frac{\rho_{d,0}}{(r/r_b)^\gamma (1 + (r/r_b)^2)^{(3-\gamma)/2}} \quad (1)$$

which closely describes a Navarro, Frenk & White¹⁵ profile for $\gamma = 1$, and has the typical asymptotic behavior at large radii found from numerical simulations of dark matter halos $\propto r^{-3}$ (e.g. Ghigna et al. 2000). See TK02 for further discussion of this model.

In addition, we assume an Osipkov-Merritt parametrization of the anisotropy β of the luminous mass distribution $\beta(r) = 1 - \frac{\sigma_\theta^2}{\sigma_r^2} = \frac{r^2}{r^2 + r_i^2}$, where σ_θ and σ_r are the tangential and radial component of the velocity dispersion and r_i is called the anisotropy radius (Osipkov¹⁶; Merritt^{12,13}). The line-of-sight velocity dispersion is found solving the spherical Jeans equation. Finally, the luminosity-weighted average within the spectroscopic aperture is computed for comparison with the observations.

2.2 Results

The effective radius and the total mass (M_E) within the Einstein radius are fixed by the observations. This leaves four free parameters in the model: the inner slope (γ) of the dark matter halo, the length scale of the dark matter component (r_b), the mass-to-light ratio of the luminous component (M_*/L_B) and the anisotropy radius (r_i). The effect of changing r_i on the model velocity dispersion is marginal and therefore r_i can be fixed to R_e . Also, according to the CDM simulations given in Bullock et al. ², the scale radius r_b is much larger than the Einstein Radius, so we will consider this limit. Hence effectively there are two free parameters which we can constrain with our observations. The results are discussed in detail in KT02 and TK02, here we

only briefly summarize the highlights: (i) MG2016+112 is a massive E/S0 and a dark cluster as suggested by Hattori et al.⁶ is therefore not necessary to reproduce the image separation; (ii) the offset from the local FP shows that the evolution of M/L for MG2016+112 is intermediate between the extrapolation of the evolution found for cluster and field samples (Fig.1), and with the independent estimate from our two-component (dark+luminous) dynamical model; (iii) dark matter contributes more than 60% (99% CL) of the total mass within the Einstein Radius; (iv) the effective slope of the *total* mass distribution is very close to isothermal, i. e. $\rho \propto r^{-\gamma'}$ with $\gamma' = 2.0 \pm 0.1 \pm 0.1$, which could be interpreted as a possible indication of (incomplete) violent relaxation; (v) the inner slope γ of the dark matter halo is flatter than isothermal ($\gamma < 2.0$; 95 % CL); (vi) using a simple adiabatic contraction model (Blumenthal et al.¹) we compute the inner slope, γ_i , before baryonic collapse and find that $\gamma_i < 1.4$ (68% CL), thus marginally inconsistent with high resolution CDM numerical simulations (Moore et al.¹⁴).

Note that the uncertainty on the slope of total mass profile is the main source of uncertainty in the determination of H_0 from gravitational time-delays (e.g Koopmans & Fassnacht¹⁰). Therefore, if what we find for MG2016 – i.e. that the total mass profile is almost perfectly isothermal – is found also for other E/S0 (see e.g. KT02b), this would lead to significant improvement in the accuracy of H_0 determination from gravitational time-delays.

Acknowledgments

We acknowledge financial support from NSF and HST grants (AST-9900866; STScI-GO 06543.03-95A; STScI-AR-09222).

References

1. Blumenthal, G. R., Faber, S. M., Flores, R., Primack, J. R., ApJ, 301, 27 (1986)
2. Bullock, J. S., et al. MNRAS, 321, 598 (2001)
3. Djorgovski S. G., Davis M., ApJ, 313, 59 (1987)
4. Dressler, A. et al. ApJ, 313, 42 (1987)
5. Ghigna, S., et al., ApJ, 544, 616 (2000)
6. Hattori M. et al., Nature, 388, 148, (1997)
7. Hernquist, L., ApJ, 356, 359 (1990)
8. Koopmans, L. V. E. & Treu, T., ApJ, 568, L5 (2002) [KT02a]
9. Koopmans, L. V. E. & Treu, T., ApJ, submitted, astro-ph/0205281 (2002) [KT02b]
10. Koopmans, L. V. E. & Fassnacht, C. D., 1999, ApJ, 527, 513
11. Koopmans, L. V. E., et al., MNRAS, in press (2002) [K02]
12. Merritt, D. 1985a, AJ, 90, 1027
13. Merritt, D. 1985b, MNRAS, 214, 25
14. Moore, B., Governato, F., Quinn, T., Stadel, J. & Lake, G., ApJ, 499, L5 (1998)
15. Navarro, J, Frenk, C. S., & White S. D. M, ApJ, 490, 493 (1997) [NFW]
16. Osipkov L. .P., 1979, Pis'ma Astron. Zh., 5, 77
17. Treu, T. & Koopmans, L. V. E. ApJ, 575, in press (2002) [TK02]
18. Treu, T., Stiavelli, M., Bertin G., Casertano, C., & Møller, P., MNRAS, 326, 237 (2001)
19. Treu, T., Stiavelli, M., Casertano, C., Møller, P., & Bertin, G., ApJ, 564, L13 (2002)